

## Nematic State of Pnictides Stabilized by Interplay between Spin, Orbital, and Lattice Degrees of Freedom

Shuhua Liang,<sup>1,2</sup> Adriana Moreo,<sup>1,2</sup> and Elbio Dagotto<sup>1,2</sup>

<sup>1</sup>*Department of Physics and Astronomy, University of Tennessee, Knoxville, Tennessee 37966, USA*

<sup>2</sup>*Materials Science and Technology Division, Oak Ridge National Laboratory, Oak Ridge, Tennessee 37831, USA*

(Received 7 May 2013; published 24 July 2013)

The nematic state of the iron-based superconductors is studied in the undoped limit of the three-orbital ( $xz$ ,  $yz$ ,  $xy$ ) spin-fermion model via the introduction of lattice degrees of freedom. Monte Carlo simulations show that in order to stabilize the experimentally observed lattice distortion and nematic order, and to reproduce photoemission experiments, *both* the spin-lattice and orbital-lattice couplings are needed. The interplay between their respective coupling strengths regulates the separation between the structural and Néel transition temperatures. Experimental results for the temperature dependence of the resistivity anisotropy and the angle-resolved photoemission orbital spectral weight are reproduced by the present numerical simulations.

DOI: [10.1103/PhysRevLett.111.047004](https://doi.org/10.1103/PhysRevLett.111.047004)

PACS numbers: 74.70.Xa, 71.10.Fd, 74.25.-q

**Introduction.**—The discovery of high temperature superconductivity in the iron-based pnictides and selenides has provided a novel playground where several simultaneously active degrees of freedom (DOF) determine the complex properties of these materials [1,2]. The mechanism that leads to superconductivity in these compounds will only be fully understood once the spin, orbital, lattice, and charge are all together considered in a consistent theory. The parent compounds of most pnictides become antiferromagnetic (AFM) at a Néel temperature  $T_N$  where long-range collinear spin order develops with wave vector  $(\pi, 0)$  in the iron sublattice notation [2], breaking rotational symmetry from  $C_4$  to  $C_2$ . This state is also characterized by an orthorhombic ( $\mathcal{O}_{\text{rth}}$ ) lattice distortion with the longer (shorter) lattice constant along the AFM [ferromagnetic (FM)] direction and by the ferro-order of the  $d_{xz}$  and  $d_{yz}$  orbitals that otherwise would be degenerate [1]. In materials such as the undoped 122 compounds, the structural and magnetic transitions occur at the same temperature. However, neutron studies performed on  $\text{LaO}_{1-x}\text{F}_x\text{FeAs}$  [2] indicate that the AFM transition can be preceded by a structural transition at a temperature  $T_S > T_N$  [3,4].

There are two main proposals to explain these results. (i) In one scenario, the magnetic interactions play the key role [5–9]. In this context, the “nematic” state [10] at  $T_S$  is induced by breaking the  $Z_2$  symmetry that links the otherwise degenerate  $(\pi, 0)$  and  $(0, \pi)$  collinear states, while at  $T_N$  the remaining  $O(3)$  symmetry is broken. However, explicit Monte Carlo (MC) calculations using purely spin models [11,12] revealed only a tiny difference between the two critical temperatures. This suggests that other DOF may be needed to reinforce the nematicity mechanism since recent experiments revealed a nematic transition well above  $T_N$  for  $\text{BaFe}_2\text{As}_2$  [13] and  $\text{NaFeAs}$  [14] that persists into the doped regime far from magnetic transitions. (ii) In another scenario, orbital fluctuations are the

crucial component [15–21], similarly as in the manganites where orbital order occurs well above the magnetic critical temperatures [22].

Both approaches explain some of the experimental data, but in practice it is difficult to disentangle the “driver” and “passenger” roles of the different DOF. The electron acoustic-phonon coupling responsible for standard tetragonal-orthorhombic structural transitions naively appears ruled out as a relevant DOF because  $\delta = [(a_x - a_y)/(a_x + a_y)] \approx 0.003$  in the pnictides [19,20,23] ( $a_x, a_y =$  lattice constants), and this  $\delta$  is considered too small to produce the sizable anisotropies experimentally observed [13,23].

The purpose of this Letter is to revisit the influence of the lattice DOF in the pnictides via its introduction into the spin-fermion (SF) model for these materials [24–26]. This model phenomenologically considers the growing body of experimental evidence that requires a mixture of itinerant and localized DOF to properly address the iron superconductors [2,27,28]. Here, the itinerant sector will involve electrons in the  $xz$ ,  $yz$ , and  $xy$   $d$  orbitals [29]. The localized spins represent the spin of the other  $d$  orbitals [24,25] or alternatively, in a Landau-Ginzburg context, the magnetic order parameter. To our knowledge, this is the first time that all these ingredients are simultaneously studied, and the complexity of the problem requires a computational analysis. Moreover, our numerical approach also allows us to study temperatures above  $T_S$  where all DOF develop only short-range fluctuations [7,30], a regime difficult to reach by standard mean-field procedures. Our main result is that a complete description of the phenomenology of the undoped Fe-based superconductors requires the simultaneous presence of both the spin- and orbital-lattice couplings, suggesting a degree of complexity in these materials that was not previously anticipated [31].

*Model and method.*—The lattice SF model considered here is based on the purely electronic model studied before [24–26] supplemented by the coupling to the lattice:

$$H_{\text{SF}} = H_{\text{Hopp}} + H_{\text{Hund}} + H_{\text{Heis}} + H_{\text{SL}} + H_{\text{OL}} + H_{\text{Stiff}}. \quad (1)$$

This (lengthy) full Hamiltonian is written explicitly in the Supplemental Material [32].  $H_{\text{Hopp}}$  is the Fe-Fe hopping of electrons with the amplitudes selected in previous publications to reproduce angle-resolved photoemission (ARPES) results [the specific hopping amplitudes used here can be read in Eqs. (1)–(3) and Table I of Ref. [29]]. The average number of electrons per itinerant orbital is  $n = 4/3$  [29]. Our focus on the undoped case is justified: this limit already contains the physics under discussion, calculations are simpler than for the doped case, and the quenched disordering effect of chemical doping is avoided. The Hund interaction is canonical:  $H_{\text{Hund}} = -J_H \sum_{\mathbf{i}, \alpha} \mathbf{S}_{\mathbf{i}} \cdot \mathbf{s}_{\mathbf{i}, \alpha}$ , with  $\mathbf{S}_{\mathbf{i}}$  ( $\mathbf{s}_{\mathbf{i}, \alpha}$ ) the localized (itinerant with orbital index  $\alpha$ ) spin.  $H_{\text{Heis}}$  is the Heisenberg interaction among the localized spins involving nearest neighbors (NN) and next-NN interactions with couplings  $J_{\text{NN}}$  and  $J_{\text{NNN}}$ , respectively, and a ratio  $J_{\text{NNN}}/J_{\text{NN}} = 2/3$  [26] that favors collinear order (any value larger than  $1/2$  would have been equally effective).

Our emphasis will be on the coupling of spin and orbital with the structural transition. Within the spin-driven scenario, the state between  $T_N$  and  $T_S$  is characterized by short-range spin correlations  $\Psi_{\mathbf{i}} = \mathbf{S}_{\mathbf{i}} \cdot \mathbf{S}_{\mathbf{i}+\mathbf{x}} - \mathbf{S}_{\mathbf{i}} \cdot \mathbf{S}_{\mathbf{i}+\mathbf{y}}$  that satisfy  $\langle \Psi \rangle < 0$  [9], where  $\mathbf{S}_{\mathbf{i}}$  is the spin of the iron atom at site  $\mathbf{i}$  and  $\mathbf{x}, \mathbf{y}$  are unit vectors along the axes. This spin-nematic phase has been studied analytically both in strong [5,6,33] and weak coupling [8]. The  $\mathcal{O}_{\text{rth}}$  distortion  $\epsilon_{\mathbf{i}}$  associated to the elastic constant  $C_{66}$  will be considered here. This distortion is produced by coupling of lattice with the short-range magnetic fluctuations via  $H_{\text{SL}} = -g \sum_{\mathbf{i}} \Psi_{\mathbf{i}} \epsilon_{\mathbf{i}}$  [8,9,34]. Here,  $g$  is the lattice-spin coupling,  $\epsilon_{\mathbf{i}}$  is the  $\mathcal{O}_{\text{rth}}$  strain

$$\epsilon_{\mathbf{i}} = \frac{1}{4\sqrt{2}} \sum_{\nu=1}^4 (|\delta_{\mathbf{i},\nu}^y| - |\delta_{\mathbf{i},\nu}^x|), \quad (2)$$

and  $\delta_{\mathbf{i},\nu}^x$  ( $\delta_{\mathbf{i},\nu}^y$ ) is the component along  $x$  ( $y$ ) of the distance between the Fe atom at site  $\mathbf{i}$  of the lattice and one of its four neighboring As atoms that are labeled by the index  $\nu$  [35]. In this context, if the atoms could not move, the structural distortion would not occur but the  $C_4$  symmetry would still spontaneously break at a temperature  $T^* > T_N$ , leading to an anisotropic resistivity [23]. The spin in  $H_{\text{SL}}$  will only be the localized spin for computational simplicity. From the other perspective, the orbital fluctuation theory attributes the structural transition to the coupling of the lattice to the  $\mathcal{O}_{\text{rth}}$  quadrupole operator via  $H_{\text{OL}} = \lambda \sum_{\mathbf{i}} \Phi_{\mathbf{i}} \epsilon_{\mathbf{i}}$ . Here,  $\lambda$  is the orbital-lattice coupling,  $\Phi_{\mathbf{i}} = n_{\mathbf{i},x_z} - n_{\mathbf{i},y_z}$  is the orbital order parameter, and  $n_{\mathbf{i},\alpha}$  the electronic density at site  $\mathbf{i}$  and orbital  $\alpha$  [19,20].

Finally,  $H_{\text{Stiff}}$  is

$$H_{\text{Stiff}} = \frac{1}{2} k \sum_{\mathbf{i}} \sum_{\nu=1}^4 (|\mathbf{R}_{\text{Fe-As}}^{\mathbf{i}\nu}| - R_0)^2 + k' \sum_{\langle \mathbf{i}\mathbf{j} \rangle} \left[ \left( \frac{a_0}{R_{\text{Fe-Fe}}^{\mathbf{i}\mathbf{j}}} \right)^{12} - 2 \left( \frac{a_0}{R_{\text{Fe-Fe}}^{\mathbf{i}\mathbf{j}}} \right)^6 \right]. \quad (3)$$

The first term in Eq. (3) is the standard harmonic energy. The second term contains anharmonic contributions to improve the simulations' convergence [36].

Only the  $\mathcal{O}_{\text{rth}}$  distortion is considered here since our aim is to study the structural transition of the parent compounds [20]. In equilibrium, the Fe atoms form a square lattice with sites labeled by  $\mathbf{i}$  and with lattice parameter  $a_0$ ; the As atoms are at the center of each plaquette, identified with the indices  $(\mathbf{i}, \nu)$ , with coordinate  $z = \pm a_0/2$  in alternating plaquettes so that the Fe-As equilibrium distance is  $R_0 = \sqrt{3}a_0/2$ . In our study, each As atom is allowed to move in the  $x$ - $y$  plane to a new position  $\mathbf{R}_{\text{Fe-As}}^{\mathbf{i}\nu} = (\delta_{\mathbf{i},\nu}^x, \delta_{\mathbf{i},\nu}^y, \pm a_0/2)$  with respect to the Fe atom that was at site  $\mathbf{i}$  when in equilibrium. The distance between Fe atoms  $R_{\text{Fe-Fe}}^{\mathbf{i}\mathbf{j}}$  is determined *globally* via the variables  $a_x$  and  $a_y$ , both equal to  $a_0$  when in equilibrium, satisfying the constraints  $2Na_x = \sum_{\mathbf{i}=1}^N \sum_{\nu} |\delta_{\mathbf{i},\nu}^x|$  and  $2Na_y = \sum_{\mathbf{i}=1}^N \sum_{\nu} |\delta_{\mathbf{i},\nu}^y|$ , where  $N$  is the number of sites and  $\nu = 1, \dots, 4$  are the four As atoms connected to each Fe. Note that this procedure is qualitatively different from studies of Jahn-Teller distortions in Mn oxides where the Mn-Mn distance was fixed [22], while here the Fe-Fe distances can change due to the  $\mathcal{O}_{\text{rth}}$  distortion, leading to the global adjustments in lattice spacings.

The Hamiltonian is here studied via a standard MC simulation in the classical (a) localized spins  $\mathbf{S}_{\mathbf{i}}$  and (b) atomic displacements  $\delta_{\mathbf{i},\nu}^x$  and  $\delta_{\mathbf{i},\nu}^y$ . For each MC configuration of spins and atomic positions, the fermionic quantum Hamiltonian is diagonalized via library subroutines, as extensively discussed in the manganite context [22], rendering the study computationally demanding.

*Results.*—The MC simulations were performed on  $8 \times 8$  square clusters using “twisted boundary conditions” that effectively reduce finite size effects, as discussed before [26]. Typically, 8000 MC steps were used for thermalization and 50 000–100 000 steps for measurements at each temperature  $T$  and for each set of parameters. The Hund interaction was set to  $J_H = 0.1$  eV, and the classical Heisenberg couplings to  $J_{\text{NN}} = 0.012$  eV and  $J_{\text{NNN}} = 0.008$  eV, similarly as in Ref. [26]. Fixing some parameters to values used in previous investigations simplifies the analysis and allow us to focus on the effects of the lattice into a previously studied system. The stiffness constants were selected so that the dimensionless couplings  $\tilde{\lambda} = (2\lambda/kW)$  and  $\tilde{g} = (2g/kW)$  [22] are experimentally realistic [37] ( $W =$  fermionic bandwidth). Calculations indicate that both parameters should be smaller than 1 in

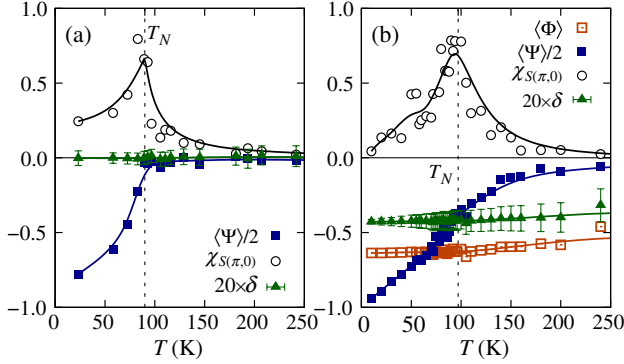


FIG. 1 (color online). Spin magnetic susceptibility  $\chi_{S(\pi,0)}$  (circles), spin-nematic order parameter  $\langle \Psi \rangle$  (filled squares), and lattice distortion  $\delta$  (triangles) vs  $T$  at  $\tilde{g} = 0$  and (a)  $\tilde{\lambda} = 0.12$  and (b)  $\tilde{\lambda} = 1.2$ . (In the latter, open squares indicate orbital order.)  $T_N$  is indicated by the dashed line.

pnictides [7,19,20,38]. The magnetic transition will be determined by the magnetic susceptibility

$$\chi_{S(\pi,0)} = N\beta \langle S(\pi,0) - \langle S(\pi,0) \rangle \rangle^2, \quad (4)$$

where  $\beta = 1/k_B T$ ,  $N$  is the number of lattice sites, and  $S(\pi,0)$  is the magnetic structure factor [at the wave vector  $(\pi,0)$  of relevance in pnictides] obtained via the Fourier transform of the real-space spin-spin correlations measured during the simulations. The structural transition is determined by the behavior of the lattice susceptibility defined by  $\chi_\delta = N\beta \langle \delta - \langle \delta \rangle \rangle^2$ , where  $\delta = ((a_x - a_y)/(a_x + a_y))$ .

*Individual couplings.*—To isolate the individual roles that the spin and orbital DOF play in their interaction with the lattice, first the case  $\tilde{g} = 0$  was studied, varying  $T$  at several values of  $\tilde{\lambda}$ . At  $\tilde{\lambda} = 0.12$ , neither a sizable lattice distortion [as indicated by the triangles in Fig. 1(a)] nor orbital order were observed, and only a Néel transition at  $T_N = 90$  K into a collinear AFM  $(\pi,0)$  state was found (see the circles in the figure). To develop a more robust lattice distortion,  $\tilde{\lambda}$  must be increased to unphysical large values. In fact, numerically it was observed that by varying  $\tilde{\lambda}$  the orbital order and structural distortion are stabilized for  $\tilde{\lambda} > 0.8$ . However, in this  $\tilde{\lambda}$  regime, already larger than estimations [19,38], the  $\mathcal{O}_{\text{rth}}$  distortion has the longest lattice constant along the FM direction [see Fig. 1(b) at  $\tilde{\lambda} = 1.2$ ], qualitatively opposite to experimental observations [39]. As a consequence, in our model, which relies on a particular set of hopping amplitudes chosen to fit ARPES experiments, the physical  $\mathcal{O}_{\text{rth}}$  or magnetic state of pnictides cannot arise from short-range orbital fluctuations alone [20]. Let us study next the role played by the spin-lattice coupling by setting instead  $\tilde{\lambda} = 0$  and focusing on, e.g.,  $\tilde{g} = 0.16$ . In this case, a peak in  $\chi_\delta$  [see Fig. 2(a)] denotes a structural transition. This transition now has the experimentally correct  $\mathcal{O}_{\text{rth}}$  distortion below  $T_N$ , i.e.,  $\delta > 0$ , and it occurs simultaneously with the Néel

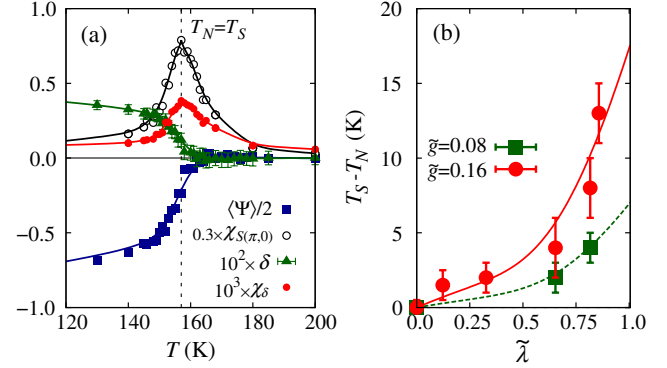


FIG. 2 (color online). (a) Spin magnetic susceptibility  $\chi_{S(\pi,0)}$  (open circles), lattice distortion susceptibility  $\chi_\delta$  (filled circles), spin-nematic order parameter  $\langle \Psi \rangle$  (squares), and lattice distortion  $\delta$  (triangles) vs  $T$  for couplings  $\tilde{g} = 0.16$  and  $\tilde{\lambda} = 0$ .  $T_N$  and the structural transition temperature  $T_S$  are indicated by the dashed line. (b) The temperature difference between  $T_S$  and  $T_N$  vs  $\tilde{\lambda}$ , at  $\tilde{g} = 0.08$  and  $0.16$ .

transition at  $T_S = T_N = 153$  K. The ordered phase now has both long-range magnetic order and a long-range  $\mathcal{O}_{\text{rth}}$  distortion with  $\delta = (a_x - a_y)/(a_x + a_y) \approx 0.0037$  (green triangles), remarkably close to experiments, suggesting that the small couplings to the lattice considered here are physically reasonable. However, setting  $\tilde{\lambda} = 0$ , no orbital order was observed, at least with the hopping amplitudes employed here. Moreover, our study shows that  $T_N$  remains equal (within the accuracy of our effort) to  $T_S$  in the physical regime, contrary to experiments. Then, neither the limits  $\tilde{\lambda} = 0$  nor  $\tilde{g} = 0$  are sufficient to fully accommodate the phenomenology of the pnictides.

*Combined couplings.*—Our main result is that the *combined* effect of the coupling of the lattice to both spins and

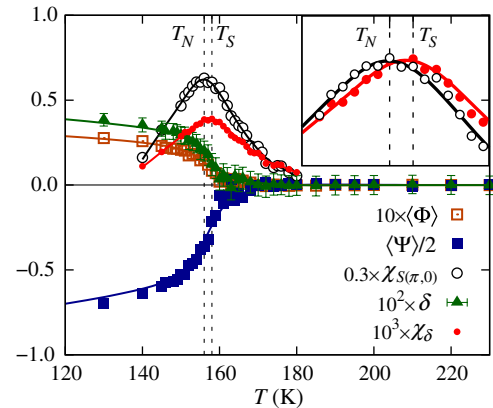


FIG. 3 (color online). Spin magnetic susceptibility  $\chi_{S(\pi,0)}$  (open circles), lattice distortion susceptibility  $\chi_\delta$  (filled circles), spin-nematic order parameter  $\langle \Psi \rangle$  (filled squares), orbital order  $\langle \Phi \rangle$  (open squares), and lattice distortion  $\delta$  (triangles) vs  $T$  at couplings  $\tilde{g} = 0.16$  and  $\tilde{\lambda} = 0.12$ .  $T_N$  and  $T_S$  are indicated by the dashed lines. Inset: close-up of the  $\chi_{S(\pi,0)}$  and  $\chi_\delta$  peaks, shifted vertically for better comparison.

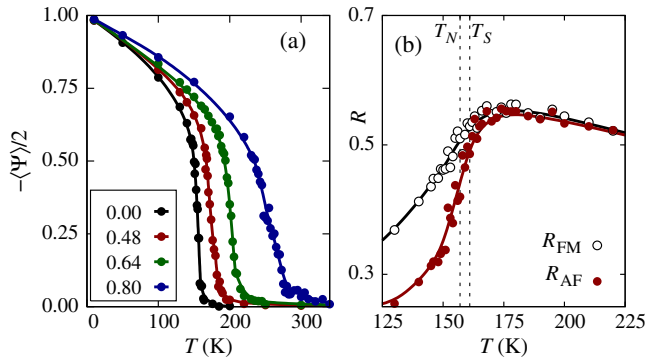


FIG. 4 (color online). (a) Spin-nematic order parameter  $\langle \Psi \rangle$  vs  $T$  at  $\tilde{g} = 0.16$  and for the values of  $\tilde{\lambda}$  indicated. (b) MC resistance along the  $x$  (AFM) and  $y$  (FM) directions varying  $T$ . Dashed lines indicate  $T_N$  and  $T_S$  at  $\tilde{g} = 0.16$  and  $\tilde{\lambda} = 0.12$ .

orbitals is needed to reach a regime with all the characteristics of the states found experimentally in pnictides. By turning on both the spin- and orbital-lattice interactions, our MC studies show that the structural transition moves to a temperature higher than the magnetic transition, so that  $T_S > T_N$ , as shown in Fig. 2(b) at  $\tilde{g} = 0.16$  and 0.08. For small couplings in the experimental range, such as  $\tilde{\lambda} = 0.12$  and  $\tilde{g} = 0.16$ , the difference  $T_S - T_N$  is concomitantly small but it is numerically clear, with  $\chi_\delta$  systematically above (below)  $\chi_{S(\pi,0)}$  at temperatures above (below) the critical region. More specifically,  $T_N = 156$  K from the peak in  $\chi_S$  (open black circles) in Fig. 3, and  $T_S = 158$  K from the peak in  $\chi_\delta$  (filled circles). The difference in the position of the two maxima (see inset) has been extensively analyzed, repeating MC runs with different starting configurations and statistics, and it appears robust. Moreover,  $T_S - T_N$  can be further enhanced by increasing  $\tilde{\lambda}$  [see Figs. 2(b) and 9 of Ref. [32]] [40]. The intermediate phase has a broken  $Z_2$  symmetry with short-range NN spin-spin correlations characterized by  $\langle \Psi \rangle < 0$ , indicating spin-nematic order (filled squares),  $\delta > 0$  indicating  $\mathcal{O}_{\text{rth}}$  distortion (triangles), and  $\langle \Phi \rangle > 0$  indicating orbital order (open squares).

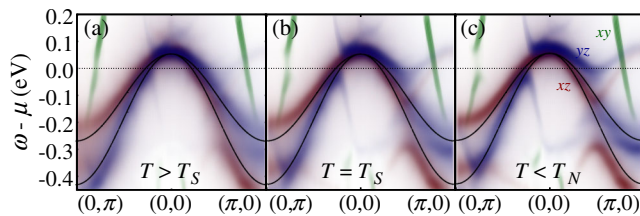


FIG. 5 (color online). Orbital-resolved spectral weight of the SF model along the directions  $(0, \pi) - (0, 0) - (\pi, 0)$  in momentum space for (a)  $T = 165$  K, (b)  $T = 158$  K, and (c)  $T = 145$  K, at  $\tilde{g} = 0.16$  and  $\tilde{\lambda} = 0.12$ . The noninteracting band dispersion is indicated by the solid black lines. The spectral weight for the  $d_{xz}$ ,  $d_{yz}$ , and  $d_{xy}$  orbitals is indicated by the red, blue, and green dots, respectively.

The order of the transitions was also investigated. In Fig. 4(a), the spin-nematic order parameter  $\langle \Psi \rangle$  is shown varying  $T$  at several  $\tilde{\lambda}$ 's and fixed  $\tilde{g} = 0.16$ . At small  $\tilde{\lambda}$ , where  $T_N = T_S$  according to Fig. 2(a), the transition is abrupt as in a first-order transition. Upon increasing  $\tilde{\lambda}$ , leading to  $T_S > T_N$ , the transition becomes continuous as in a second-order transition. This is in agreement with predictions of an effective low-energy model [8].

*Comparison with experiments.*—As in the previous effort employing the purely electronic SF model [26], the resistance  $R$  along the AFM and FM directions was calculated varying  $T$ . While the reproduction of the uniaxial-pressure experimental results [23] required previously an explicit anisotropy in the Heisenberg couplings to mimic strain, now the asymmetry develops *spontaneously* as shown in Fig. 4(b).  $R$  along the FM direction becomes larger than along the AFM direction at  $T \approx T_S$ , suggesting that the anisotropy observed above  $T_S$  in experiments may be due to the external strain [41,42].

Our study also reproduces the ARPES experiments [43–45] where an asymmetry develops between the spectral weight for the  $xz$  and  $yz$  orbitals along the  $\Gamma$ - $X$  and the  $\Gamma$ - $Y$  directions upon cooling. In Fig. 5, it is shown that along the  $\Gamma$ - $X$  [ $\Gamma$ - $Y$ ] direction, mainly near  $(\pi, 0)$  [ $(0, \pi)$ ], the spectral weight for the  $yz$  ( $xz$ ) orbital moves closer to (further from) the Fermi level as  $T$  is lowered, compatible with the development of orbital order with  $\langle \Phi \rangle > 0$ . The asymmetry is obtained here without explicit symmetry breaking at the Hamiltonian level [46]. Note also that orbital order may only occur near the Fermi surface [47]. It is important to remark that in spite of the small values of  $\tilde{\lambda}$  and  $\tilde{g}$  used in our effort, their influence is sufficient to create observable consequences such as the anisotropies in transport and ARPES. In addition, a recent pair-distribution function analysis reported the presence of robust *local*  $\mathcal{O}_{\text{rth}}$  distortions [48], hinting that the lattice DOF is more important than previously believed [49].

*Conclusions.*—In the model analyzed here, the couplings of the spin and orbital DOF with the lattice are *both* important to stabilize the state that breaks the  $C_4$  symmetry above the Néel transition. The spin-lattice coupling induces the correct experimentally observed  $\mathcal{O}_{\text{rth}}$  distortion, while the orbital-lattice coupling generates the ARPES-observed orbital order and the higher temperature structural transition. As a consequence, our study suggests that the complex nematic properties of the pnictides' parent compounds arise from a subtle cooperation among all the participating degrees of freedom.

This work was supported by the U.S. Department of Energy, Office of Basic Energy Sciences, Materials Sciences and Engineering Division.

- [1] D. C. Johnston, *Adv. Phys.* **59**, 803 (2010).
- [2] P. Dai, J.-P. Hu, and E. Dagotto, *Nat. Phys.* **8**, 709 (2012).

- [3] R. M. Fernandes, D. K. Pratt, W. Tian, J. Zarestky, A. Kreyssig, S. Nandi, M. G. Kim, A. Thaler, N. Ni, P. C. Canfield, R. J. McQueeney, J. Schmalian, and A. I. Goldman, *Phys. Rev. B* **81**, 140501(R) (2010).
- [4] S. Nandi, M. G. Kim, A. Kreyssig, R. M. Fernandes, D. K. Pratt, A. Thaler, N. Ni, S. L. Bud'ko, P. C. Canfield, J. Schmalian, R. J. McQueeney, and A. I. Goldman, *Phys. Rev. Lett.* **104**, 057006 (2010).
- [5] C. Fang, H. Yao, W.-F. Tsai, J. P. Hu, and S. A. Kivelson, *Phys. Rev. B* **77**, 224509 (2008).
- [6] C. Xu, M. Müller, and S. Sachdev, *Phys. Rev. B* **78**, 020501(R) (2008).
- [7] R. M. Fernandes, L. H. VanBebber, S. Bhattacharya, P. Chandra, V. Keppens, D. Mandrus, M. A. McGuire, B. C. Sales, A. S. Sefat, and J. Schmalian, *Phys. Rev. Lett.* **105**, 157003 (2010).
- [8] R. M. Fernandes, A. V. Chubukov, J. Knolle, I. Eremin, and J. Schmalian, *Phys. Rev. B* **85**, 024534 (2012).
- [9] R. M. Fernandes and J. Schmalian, *Supercond. Sci. Technol.* **25**, 084005 (2012).
- [10] E. Fradkin, S. A. Kivelson, M. J. Lawler, J. P. Eisenstein, and A. P. Mackenzie, *Annu. Rev. Condens. Matter Phys.* **1**, 153 (2010).
- [11] Y. Kamiya, N. Kawashima, and C. D. Batista, *Phys. Rev. B* **84**, 214429 (2011).
- [12] A. L. Wysocki, K. D. Belashchenko, and V. P. Antropov, *Nat. Phys.* **7**, 485 (2011).
- [13] S. Kasahara, H. J. Shi, K. Hashimoto, S. Tonegawa, Y. Mizukami, T. Shibauchi, K. Sugimoto, T. Fukuda, T. Terashima, A. H. Nevidomskyy, and Y. Matsuda, *Nature (London)* **486**, 382 (2012).
- [14] A. F. Wang *et al.*, *New J. Phys.* **15**, 043048 (2013).
- [15] C.-C. Lee, W.-G. Yin, and W. Ku, *Phys. Rev. Lett.* **103**, 267001 (2009).
- [16] C.-C. Chen, B. Moritz, J. van den Brink, T. P. Devereaux, and R. R. P. Singh, *Phys. Rev. B* **80**, 180418(R) (2009).
- [17] W. Lv, J. S. Wu, and P. Phillips, *Phys. Rev. B* **80**, 224506 (2009).
- [18] C.-C. Chen, J. Maciejko, A. P. Sorini, B. Moritz, R. R. P. Singh, and T. P. Devereaux, *Phys. Rev. B* **82**, 100504(R) (2010).
- [19] H. Kontani, Y. Inoue, T. Saito, Y. Yamakawa, and S. Onari, *Solid State Commun.* **152**, 718 (2012).
- [20] H. Kontani, T. Saito, and S. Onari, *Phys. Rev. B* **84**, 024528 (2011).
- [21] W.-C. Lee, W. Lv, J. M. Tranquada, and P. W. Phillips, *Phys. Rev. B* **86**, 094516 (2012).
- [22] E. Dagotto, T. Hotta, and A. Moreo, *Phys. Rep.* **344**, 1 (2001).
- [23] J.-H. Chu, J. G. Analytis, K. De Greve, P. L. McMahon, Z. Islam, Y. Yamamoto, and I. R. Fisher, *Science* **329**, 824 (2010); see also I. R. Fisher, L. Degiorgi, and Z. X. Shen, *Rep. Prog. Phys.* **74**, 124506 (2011).
- [24] W. Lv, F. Krüger, and P. Phillips, *Phys. Rev. B* **82**, 045125 (2010).
- [25] W.-G. Yin, C.-C. Lee, and W. Ku, *Phys. Rev. Lett.* **105**, 107004 (2010).
- [26] S. Liang, G. Alvarez, C. Sen, A. Moreo, and E. Dagotto, *Phys. Rev. Lett.* **109**, 047001 (2012).
- [27] H. Gretarsson *et al.*, *Phys. Rev. B* **84**, 100509(R) (2011).
- [28] F. Bondino *et al.*, *Phys. Rev. Lett.* **101**, 267001 (2008).
- [29] M. Daghofer, A. Nicholson, A. Moreo, and E. Dagotto, *Phys. Rev. B* **81**, 014511 (2010).
- [30] J. L. Niedziela, D. Parshall, K. A. Lokshin, A. S. Sefat, A. Alatas, and T. Egami, *Phys. Rev. B* **84**, 224305 (2011).
- [31] The far more challenging study of the effect of doping and quenched disorder is currently in progress.
- [32] See Supplemental Material at <http://link.aps.org/supplemental/10.1103/PhysRevLett.111.047004> for the details of the model and the computational technique.
- [33] Q. Si and E. Abrahams, *Phys. Rev. Lett.* **101**, 076401 (2008).
- [34] J.-H. Chu, H.-H. Kuo, J. G. Analytis, and I. R. Fisher, *Science* **337**, 710 (2012).
- [35] According to the experimental results, it is known that  $\langle \epsilon_i \rangle < 0$  if the magnetic order of the ground state is  $(\pi, 0)$  [23]. For this reason, only positive values of the spin-lattice constant  $g$  must be considered since otherwise an unphysical lattice distortion would result.
- [36] If only harmonic terms are considered for the Fe atoms, the results do not change but it takes longer to achieve numerical convergence.
- [37]  $W = 3$  eV is the bandwidth of the three-orbital model [29].
- [38] L. Boeri, O. V. Dolgov, and A. A. Golubov, *Phys. Rev. Lett.* **101**, 026403 (2008).
- [39] If in the orbital-lattice term  $H_{OL}$  a negative value of  $\epsilon$  is introduced and kept fixed, so that  $a_x > a_y$  as in experiments, a distortion of the Fermi surface that favors the intraorbital nesting along  $(0, \pi)$  is induced. Thus, changing the sign of the coupling in  $H_{OL}$  leads to the correct lattice distortion but the incorrect spin order.
- [40] Integrating out the lattice DOF in our model may lead to the three-point vertex couplings discussed by S. Onari and H. Kontani, *Phys. Rev. Lett.* **109**, 137001 (2012), where  $T_S > T_N$  is also reported.
- [41] C. Dhital, Z. Yamani, W. Tian, J. Zarestky, A. S. Sefat, Z. Wang, R. J. Birgeneau, and S. D. Wilson, *Phys. Rev. Lett.* **108**, 087001 (2012).
- [42] E. C. Blomberg *et al.*, *Phys. Rev. B* **85**, 144509 (2012).
- [43] M. Yi *et al.*, *Proc. Natl. Acad. Sci. U.S.A.* **108**, 6878 (2011).
- [44] C. He *et al.*, *Phys. Rev. Lett.* **105**, 117002 (2010).
- [45] Y. Zhang *et al.*, *Phys. Rev. B* **85**, 085121 (2012).
- [46] M. Daghofer, A. Nicholson, and A. Moreo, *Phys. Rev. B* **85**, 184515 (2012).
- [47] M. Daghofer, Q.-L. Luo, R. Yu, D. X. Yao, A. Moreo, and E. Dagotto, *Phys. Rev. B* **81**, 180514(R) (2010).
- [48] J. L. Niedziela, M. A. McGuire, and T. Egami, *Phys. Rev. B* **86**, 174113 (2012).
- [49] Similar conclusions were reached in a recent ARPES study of  $\text{Fe}_{1.02}\text{Te}$ : Z. K. Liu *et al.*, *Phys. Rev. Lett.* **110**, 037003 (2013).